Mon. Not. R. Astron. Soc. **000**, 1–15 (2003) Printed 27 June 2007 (MN LATEX style file v2.2)

Carbon abundances and $^{12}C/^{13}C$ from globular cluster giants

Yakiv V.Pavlenko[1⋆], Hugh R.A.Jones[2]† and Andrew J. Longmore[3]‡
[1] *Main Astronomical Observatory of Ukrainian Academy of Sciences, Golosiiv woods, 03680 Kyiv-127, Ukraine*
[2] *Astrophysics Research Institute, Liverpool John Moores University, Egerton Wharf, Birkenhead CH41 1LD, UK*
[3] *UK Astronomy Technology Centre, Royal Observatory Edinburgh, Blackford Hill, Edinburgh EH9 3HJ, Scotland*

Accepted 1988 December 15. Received 1988 December 14; in original form 1988 October 11

ABSTRACT

The behaviour of the $\Delta\nu$=2 CO bands around 2.3 μm was examined by comparing observed and synthetic spectra in stars in globular clusters of different metallicity. Changes in the $^{12}C/^{13}C$ isotopic ratio and the carbon abundances were investigated in stars from 3500–4900 K in the galactic globular clusters M71, M5, M3 and M13, covering the metallicity range from –0.7 to –1.6. We found relatively low carbon abundances that are not affected by the value of oxygen abundance. For most giants the $^{12}C/^{13}C$ ratios determined are consistent with the equilibrium value for the CN cycle. This suggests complete mixing on the ascent of the red giant branch, in contrast to the substantially higher values predicted across this range of parameters by the current generation of models. We found some evidence for a larger dispersion of $^{12}C/^{13}C$ in giants of M71 of metallicity [μ] = [M/H] = -0.7 in comparison with the giants of M3, M5 and M13, which are more metal deficient. Finally, we show evidence for lower $^{12}C/^{13}C$ in giants of globular clusters with lower metallicities, as predicted by theory.

Key words: evolution of globular clusters giants, carbon isotopic ratio, CO bands, infrared spectra, abundances

1 INTRODUCTION

Abundance patterns are sensitive indicators of the history of nuclear processing and mixing processes inside stars. During the main sequence phase of its lifetime, a star of mass above around 0.8 $M_\odot$ will convert ^{12}C into ^{13}C (and also ^{14}C) via the CN cycle. If material which has undergone any degree of CN cycle burning is mixed to the surface of a star, the carbon isotope ratio $^{12}C/^{13}C$ will decrease.

The equilibrium $^{12}C/^{13}C$ value for the CN cycle is $\sim$ 3.5. Standard models of the mixing occurring at the first ascent of the Pop I red giant branch find $^{12}C/^{13}C$ ratios in the range from 90 (solar value, Anders & Grevesse 1989) to 20 (see Iben 1964, Iben & Renzini 1983, Sneden et al. 1986, Charbonnel 1994). The first measurements of the $^{12}C/^{13}C$ in the atmospheres of field red giants showed lower than predicted values. Population I giants have carbon isotope ratios in the vicinity of 5–40 (Lambert & Ries 1981, see also references in Briley et al. 1997). This discrepancy cannot be explained by low initial isotope ratios (Sneden at al. 1986, Gilroy & Brown 1991).

In general, the situation with the theory of $^{12}C/^{13}C$ evolution in Pop II giants is even more problematic than for Pop I stars: results of modelling depend on metallicity. Due to the lower opacity inside these stars, they are more luminous. In general, they evolve on a shorter time scale than do Population I stars. Thus, we expect that initial $^{12}C/^{13}C$ (and carbon abundance, log N(C)) values may vary with age and thus metallicity [μ] . For our range of masses, effective temperature ($T_{\rm eff}$) and metallicities conventional theory predicts rather high ratios of $^{12}C/^{13}C > 20$ (see Fig. 4 in Boothroyd and Sackmann 1999) after both first and second dredge-up mixing. Models of the evolution of metal deficient halo stars show that the $^{12}C/^{13}C$ isotopic ratio should be slightly lower in metal-deficient stars (Charbonnel 1994).

The canonical picture of the evolution of globular cluster stars suggests that they should consist of chemically homogeneous populations of stars. In reality observations indicate that most galactic globular clusters exhibit star-to-star variations of atmospheric abundances of C,N,O, and other elements associated with proton capture reactions. Gratton et al. (2001) find some evidence that low-mass clusters are chemically more homogenous; abundances of Fe and Ca are

⋆ E-mail: yp@mao.kiev.ua
† E-mail:hraj@astro.livjm.ac.uk
‡ E-mail:ajl@roe.ac.uk

almost the same among stars of a given cluster (cf. Kraft et al. 1997; Ivans et al. 2001). However, there are two exceptions: M22 and ω Cen (cf. Vanture et al. 2002, Smith et al. 2002).

Two main explanations have been proposed for the observed CNO abundance variations (cf Kraft 1994): a) some of the stars (CN-strong stars) were formed by gas that had been pre-enriched by nitrogen and other elements during star formation by accretions of ejecta from more massive and fast evolving stars; b) observed CN enhancements are due to deep mixing processes, which have brought freshly synthesized products from interior regions of active CNO element nucleosynthesis to the stellar surface (Sweigart & Mengel 1979). Deep mixing elevates the N-rich and C (and possibly O) deficient matter from the CN (and possibly ON) cycle regions above the H-burning shell into the outer convective envelope during RGB ascent, causing corresponding changes to surface abundances.

The combined model of primordial abundance variations among the stars and deep mixing processes during the late stages of evolution seems to explain the observed abundance inhomonogeneties (Messenger & Lattanzio 2002, Ramires & Cohen 2002, Briley & Cohen 2001, Briley et al. 2001). The solution to this problem is complicated by the fact that similar chains of nuclear reactions, i.e. proton captures by C,N,O, Ne and Mg are associated with both mechanisms (see Briley et al. 2002 for more details).

Therefore determinations of $^{12}C/^{13}C$ can play a key role in improving our knowledge about the evolution of globular clusters giants. Specifically, observations of the $^{12}C/^{13}C$ isotope ratio should allow us to pinpoint the evolutionary phase at which mixing occurs. Isotope ratios in stars with a range of metallicity can give us information about the role of metal abundance in suppressing or enhancing mixing. Previous work concentrated on halo giants, showing that carbon isotope ratios in metal poor stars decline abruptly to very low values at log g $\sim$ 2 on the first ascent of the giant branch (Sneden et al. 1986; Pilachowski et al. 1997). Pilachowski et al. (1997) also found weak evidence for a continuing decline in carbon isotope ratio with increasing luminosity in metal poor giants from log g = 2 to 0. Although previous studies benefit from field stars being relatively brighter there are a couple of advantages to studying globular cluster giants. Firstly relative to field giants, globular cluster giants can be expected to have arisen from similar composition material and thus should be composed of more homogeneous material. Secondly, stars in a particular cluster can be considered to be at a common distance (the diameter of a globular cluster being negligible in comparison to the distance from us). Thus their distances are better determined than the distances of field halo giants.

In this paper, carbon isotope ratios of 28 relatively well studied red giant stars taken from globular clusters with a range of metallicities[1] $[\mu]$ = [M/H] = $[Fe/H]_*$–$[Fe/H]_\odot$ = –0.7 (M71) to $[\mu]$ = –1.6 (M3) were investigated. Section 2 describes the observations, Section 3 presents the model atmospheres and fits to the observed spectra, Section 4 is discussion and Section 5 the conclusions.

[1] In this paper the definition of metallicity is related to iron and other heavy metal abundances though not to those of carbon and oxygen.

2 OBSERVATIONS

Observations were made with the Cooled Grating Spectrometer 4 (CGS4) on the UK Infrared Telescope (UKIRT) on Mauna Kea, Hawaii. The instrument then had a 58 × 62 InSb array which was moved in the focal plane in order to three times over-sample the spectrum. Sky subtraction was performed by nodding the telescope approximately 30 arcsec up and down the slit, ensuring that during alternate 'object' and 'sky' observations the star remained on the detector. The observations presented in this paper were made during three nights, 1992 April 23 and 24 in a wide variety of conditions of optical seeing (0.75–2 arcsec) and of atmospheric humidity (10–75 per cent).

Observations were carried out for a sample of globular cluster stars, without detailed analysis of their membership. Our later analysis based on the literature sources has shown that at least some of the stars are non-members (see section 4).

The 150 lines mm^{-1} grating was used in third order with the 150 mm focal length camera at a central grating wavelength of 2.34μm. This grating position was chosen as it allows simultaneous coverage of the ^{12}CO and ^{13}CO band heads. This position also enabled CGS4 to work at high grating efficiency in a region of relatively high atmospheric transmission with relatively high resolution.

To remove telluric bands of water, carbon dioxide and methane, we observed A type standards. Such stars are not expected to have features in common with our target stars and are mainly featureless (Malkan et al. 2002). The airmass difference between object and standard used never exceeded 0.05 and so we are confident that the spectra have good cancellation of atmospheric features. Both the object and the standard were wavelength calibrated by using arc lines of krypton, argon and xenon and OH lines. To extract the spectrum from the sky subtracted signal an Optimal Extraction technique was used; this combines the rows using weights based on the spatial profile of the stellar image. The spectra were reduced following Jones et al. (1994) using the *Figaro*, *Specdre* and *Kappa* packages provided and supported by Starlink.

3 PROCEDURE

There are several ways of determining abundances of the CNO elements and the carbon isotopic ratio in the atmospheres of late type stars. In studies of CNO abundances, one method is to derive O abundances from atomic lines or OH bands, followed by CH bands to set [C/Fe] (Cottrell 1978). Other approaches have used CO bands at 2.3 μm (Smith & Suntzeff 1989) or CO bands at 1.6 μm (Bell & Briley 1991, Smith et al. 2002). If C and O are known, CN bands in the blue and red can be used to constrain [N/Fe] (Briley et al. 2001, 2002). Note, however, that in some studies, as in our case, O is not known and some average value must be assumed. In some cases it is possible to use NH for a direct measurement of [N/Fe] (Yakovina & Pavlenko 1998).

A self consistent approach for determination of log N(C) and $^{12}C/^{13}C$ from fits to observed spectra of OI, molecular C_2 and CN was developed by Pavlenko (1991) and Boyarchuk et al. (1991). In most cases, carbon isotope ratios can be determined from both red ^{13}CN bands and ^{13}CO bands.

3.1 Model Atmospheres and Synthetic Spectra

Model atmospheres were computed using the SAM12 program (Pavlenko 2002, 2003), which is a modification of ATLAS12 (Kurucz 1999). The standard set of continuum opacities included in ATLAS12 by Kurucz (1999) is used. Computations of a few opacities were added or upgraded: the absorption of C^- (Myerscough & McDowell 1966) and H_2^- Doyle (1968). To compute opacities due to bound-free absorption of C, N, O atoms we used TOPBASE (Seaton et al. 1992) and cross-sections from Pavlenko & Zhukovska (2003). Our bound-free transition opacity tables are available on the Web (Pavlenko 2003b).

Opacities due to atomic and molecular lines absorption were taken into account using the opacity sampling approach (Sneden et al. 1976). Line list data were taken from different sources: atomic lines from VALD (Kupka et al. 1999); lines of diatomic molecules CN, C_2, CO, SiH, CO from CDROM 18 of Kurucz (1993); H_2O line list from the AMES database (Partridge & Schwenke 1998); OH line list from Schwenke (1997). TiO and VO opacities were taken into account using the JOLA approach. Algorithms for molecular band opacity computations allow reproduction of the relative strength and shapes of the spectral energy distributions for late type stars (Pavlenko 1997, 2000, 2003).

The shape of every line was determined using the Voigt function $H(a, v)$. Damping constants were taken from line databases or computed using Unsold's approach (Unsold 1955). In model atmosphere computations we adopt a microturbulent velocity, V_t , of 2 km/s. For some spectra we investigated the effect of varying V_t (see Table 4 and section 4).

The photospheres of K- and M-giants lie on the upper boundary of their convective envelopes. In fact convection determines the lower boundary conditions for the equations of energy transfer in model atmosphere computations. The mixing length theory of 1D convection modified by Kurucz(1999) is used in ATLAS12 and SAM12.

In the frame of this approach the mixing length parameter l/H should be defined. Heiter et al., (2002) find that spectroscopic measurements require 0.5, Asida (2000) derives l/H =1.4, Kurucz (1993, 1999) used l/H = 1.25. Generally speaking, the choice of l/H is rather arbitrary — it is actually a combination of different parameters often constructed with different formalisms. In that sense different headline values of mixing lengths from different models may in fact be equivalent (Salaris, Cassisi & Weiss 2002).

Two grids of model atmospheres used in this paper were computed for l/H = 2.0 and 1.4. l/H = 2.0 represents an approximate upper limit for l/H . However, our computations indicate that only the inner region of our globular cluster photospheres is sensitive to l/H (Fig. 1). Our synthetic spectra show very weak dependence: variations in S used to quantify the minimisation procedure are marginal (< 1 %) when l/H changes from 0.5 to 2.0 in the model atmospheres (Fig. 1); however, also see section 3.4.

The model atmospheres were computed in the range of T_{eff} = 3000 to 5000 K, log g = 0.0 to 2.0, $[\mu]$ = –0.5 to –2.0, and different carbon abundances log N(C). For every giant we computed 10 model atmospheres of different log N(C), with 0.2 dex as a step for log N(C). Then, for each value of log N(C) we computed a grid of synthetic spectra for the wavelength range from 2.26–2.39 μm . Synthetic spectra were computed for a grid of $^{12}C/^{13}C$ = 90, 40, 20, 10, 9, 8, 7, 6, 5, 4, 3.

In our computations the abundances of oxygen and nitrogen were fixed, i.e. log N(N)= log $N_\odot$(N) + $[\mu]$, log N(O) = log $N_\odot$(O) + $[\mu]$. To study the dependence of our results on log N(O) we carried out some numerical experiments with variable oxygen abundances (see section 3.4)

Numerical computations of theoretical radiative fluxes F_ν in spectra of red giants were carried out within the classical approach: LTE, plane-parallel model atmosphere and no energy divergence by WITA6 (Pavlenko 2000).

The spectra are calculated using a self-consistent approach: model atmospheres and synthetic spectra are computed for the same opacity source lists and sets of abundances. This approach allows us to treat the possible impact of abundance changes on the temperature structure of the model atmosphere as well as on the emitted fluxes in a direct way.

We will use a definition of 'synthetic spectra' as an alias for "theoretical spectral energy distributions of the spectrum of red giants". Computations were carried out with wavelength steps $\Delta\lambda$ = 0.05 nm and 0.01 nm (see section 3.4).

Our spectra of the second overtone bands of CO are contaminated by water lines formed inside the M-giants atmospheres. In our computations we always took into account absorption using AMES line lists of CO (Goorvitch 1994), H_2O (Partrige & Schwenke 1997) and atomic line list from VALD (Kupka et al. 1999). The reliability of the AMES lists for astrophysical computations was shown by Jones et al. 2002 and Pavlenko & Jones 2002.

3.2 Dependence on input parameters

3.2.1 Dependence on $T_{\rm eff}$

In Fig. 1 we show the temperature structure T = f(P_g) for some of our model atmospheres with different T_{eff} , log g, and $[\mu]$. Photospheres of cooler giants move downwards to more dense layers due to the overall reduction of opacity. In general, for lower T_{eff} the curves T = f(P_g) in Fig. 1 are systematically shifted toward lower temperature/higher pressure regions. A comparison of computed fluxes is shown in Fig. 2. It is worth noting:

• for T_{eff} = 3500–4500 K the overall shape of spectral energy distributions is governed by CO; larger changes are seen for T_{eff} = 4500–5000 K, these are primarily caused by differences in the temperature structure of the models (see right panel of Fig. 2).

• if T_{eff} drops below 4500 K bands of H_2O appear in the region (see Pavlenko & Jones 2002 for more details).

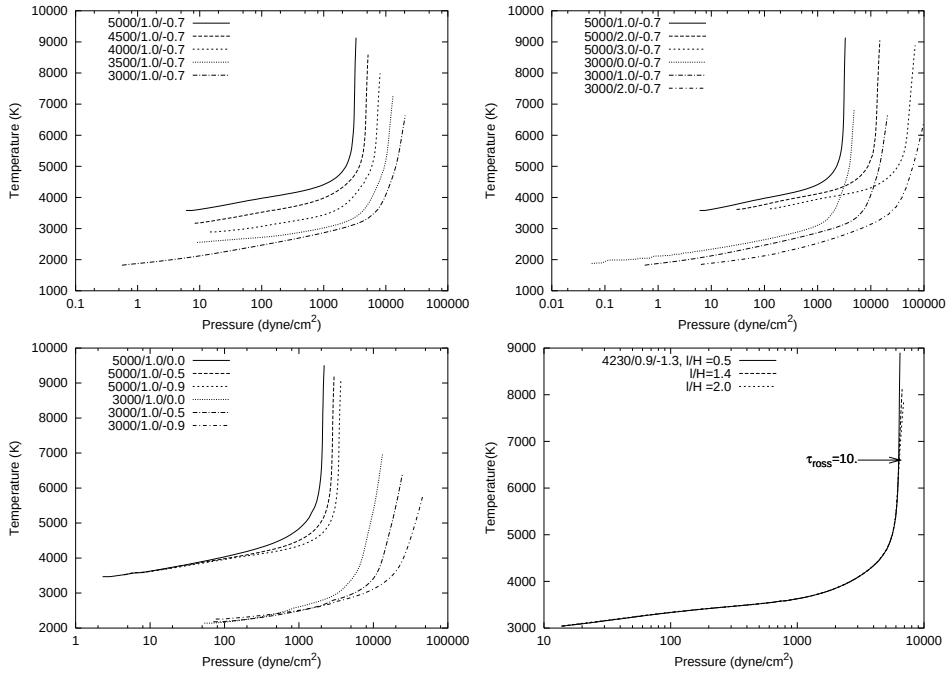

Figure 1. Temperature versus pressure in red giant model atmospheres of different $T_{\rm eff}$, log g, $[\mu]$, l/H

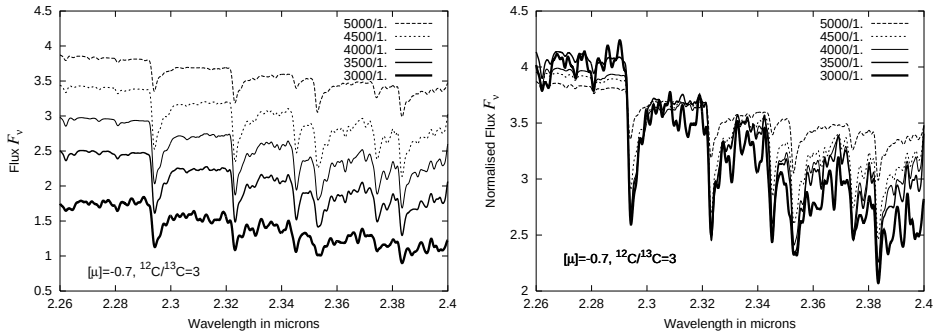

Figure 2. Left: F_ν fluxes computed for model atmospheres of $[\mu]$ = – 0.7. Right: Fluxes normalised to equal value at 2.344 μm. The regular absorption features are caused by CO bands. The smaller scale features appearing in the spectra below 4500 K are due to water vapour.

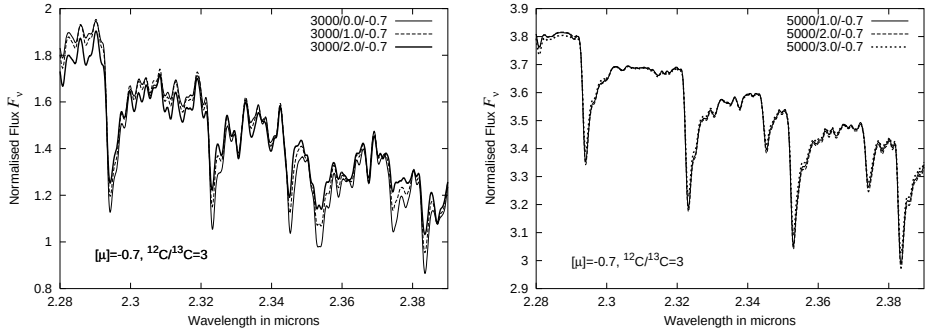

Figure 3. Synthetic spectra computed for model atmospheres of different log g — left: $T_{\rm eff}$ = 3000 K, right: $T_{\rm eff}$ = 5000 K.

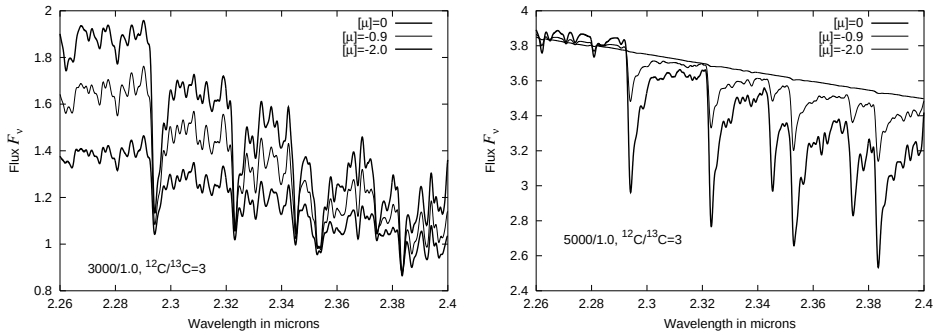

Figure 4. Synthetic spectra computed for model atmospheres of different [μ] — left: $T_{\rm eff}$ = 3000 K, right: $T_{\rm eff}$ = 5000 K.

3.2.2 Dependence on log g

Computed temperature structures T =f(P_g) of some model atmospheres of $T_{\rm eff}$ = 3000 and 5000 K and different log g are shown in Fig. 1. There is a wide range of characteristic pressure for the photospheric layers across all the models we calculated. On the other hand, the dependence on log g of our computed spectra for model atmospheres of $T_{\rm eff}$ = 5000 and 3000 is quite different (Fig. 3). Specifically, spectra computed for $T_{\rm eff}$ = 5000 K show a rather weak dependence on log g.

3.2.3 Dependence on metallicity

Small variations of [μ] ($\pm$ 0.2 dex) have little influence on the temperature structure of model atmospheres (Fig. 1). Continuum absorption governs the opacity in metal deficient atmospheres. Both CO and H_2O molecular densities are very sensitive to the [μ] parameter (Fig. 4).

3.2.4 Dependence on log N(O) and log N(C)

The chemical balance in red giant atmospheres is governed by the C/O ratio through the formation of CO and H_2O molecules (Tsuji 1973). In the atmospheres of M-giants C/O $<$ 1 and the majority of carbon atoms are bound into CO molecules. For globular cluster giants, C/O $<<$ 1. As a result, the profiles of CO bands in IR spectra of the M giants we modelled show strong sensitivity to log N(C), see Fig. 5. We used this dependence for finding log N(C) for our M giant spectra. On the other hand, the temperature structure of model atmospheres as well as the profiles and relative strengths of the computed CO bands show rather weak dependence on log N(O) (see Figs. 6), especially if log N(C) and log N(O) differ significantly, as in atmospheres of our giants. Similar results were found by Smith & Suntzeff (1989).

3.2.5 Dependence on V_t

In our analysis we use absorption lines of intermediate strength. Therefore our results should show a dependence on microturbulent velocity (cf. Smith & Suntzeff 1989). Microturbulent velocities in the atmospheres of giants of globular clusters lie in the range 1–3 km/s (see Kraft et al. 1997, Ivans et al. 2001, Ramirez and Cohen (2002, 2002a) and references therein, as well as our Table 4). We computed a few model atmospheres and synthetic spectra for metal deficient giants with different V_t (Fig. 7). In general, the dependence on V_t increases towards lower $T_{\rm eff}$. This arises because:

a) In the low temperature regime the relative contribution of microturbulent velocities to the total velocity field $V_{total} = (2 * R * T/\mu + V_t^2)^{1/2}$ increases.

b) Lower temperatures lead to the formation of many absorption lines of intermediate strength which have a strong dependence on V_t .

3.3 Choice of $T_{\rm eff}$ and log g parameters

In order to investigate the carbon abundance and isotopic ratio in the target stars it is important that other parameters can be fixed in a reliable and consistent manner. Effective temperatures and gravities for nearly all of the targets are taken from the study of Alonso et al. (1999, 2000). The empirical nature of the study, the large sample size and the use of interferometric and Hipparcos data gives us confidence that our results will not be undermined by uncertainties in radii and temperature.

3.4 Fits to observed spectra

In fitting the observational data to synthetic spectra we followed a scheme described by Jones et al. (2002) and Pavlenko & Jones (2002). In order to determine the best fit parameters for our targets in a systematic fashion, we performed a least-squared minimisation on the observed spectra within a grid of synthetic spectra smoothed to the resolution of the data using a triangular function to mimic the square pixels of the detector. Then, for every spectrum we minimised a 3D function $S = f(x_s, x_f, x_w) = 1/N \times \sum(1 - F_{obs}/F_{synt})^2$, where F_{obs}, F_{synt} are observed and computed fluxes, N is the number of points in the observed spectrum to be fitted. x_s, x_f, x_w are respectively the relative shift in wavelength scale, a normalisation factor used to overlay observed and computed spectra and an instrumental broadening parameter.

Our "best fits" for every giant of our sample are shown in the next section of the paper. All these fits were found from minimisation of the S function. In the observed region there are four band heads of ^{12}CO at 2.29, 2.32, 2.35, 2.38 μm and two of ^{13}CO at 2.345, 2.37 μm. After a number

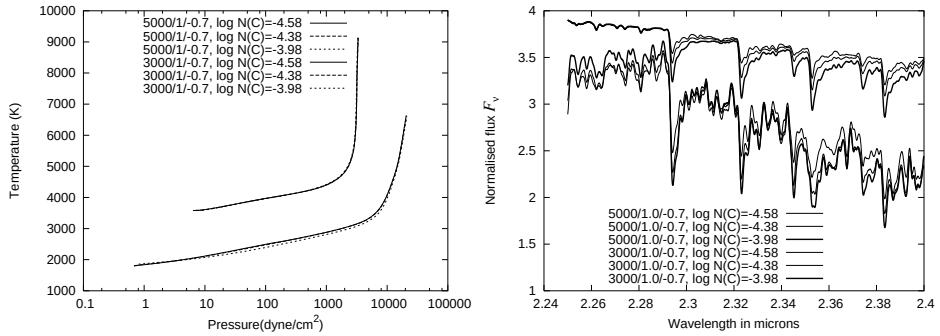

Figure 5. Computed temperature structures of model atmospheres with different log N(C) and the synthetic spectra for these model atmospheres.

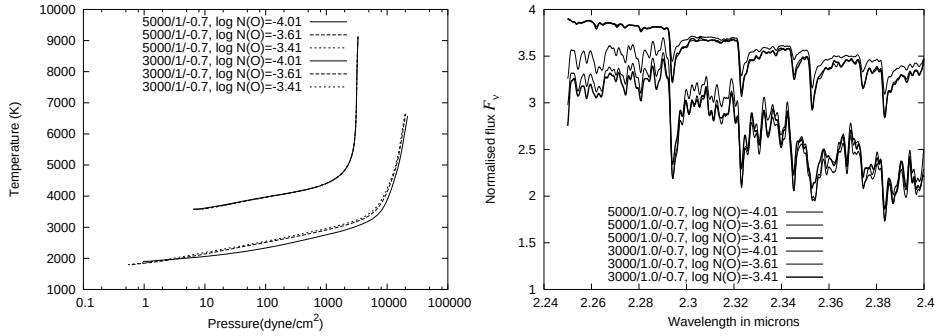

Figure 6. Computed temperature structures of model atmospheres with different log N(O) and the synthetic spectra for these model atmospheres.

of trials we found that our most reliable solutions could be found from the CO band heads in the spectral region from 2.285 – 2.36 μm. Unfortunately only one ^{13}CO band head, at 2.345 μm, lies in this region. In principle, the other band of $^{13}C^{16}O$ at 2.375 μm provides a more sensitive tool for $^{12}C/^{13}C$ determination in spectra of M-stars (see Pavlenko & Jones 2002) but our data do not cover properly the whole feature. The spectra have a slight curvature, which we correct for but which has greatest error at the edge of the array.

Fig. 8 shows two examples of fits to observed spectra using a narrow (2.285 - 2.36 μm) and wider wavelength region (2.285 - 2.38 μm). The latter contains also the 2.375 μm $^{13}C^{16}O$ band head. We note a number of features:

(1) Our computations of synthetic spectra were carried out with wavelength resolution of $\Delta\lambda = 0.01$ nm. We found that the lower wavelength resolution introduced extra computational noise, although the value of the min (S) for $\Delta\lambda$ = 0.01 nm and 0.05 nm remained the same in most cases.

(2) Since we believe the quality of the theoretical spectra is expected to be excellent throughout the modelled region we may cautiously use S to estimate the quality of the observed spectra. Our minimisation value S increases when we use the 2.375 μm band in our analysis: from our "standard" fit over 2.285 — 2.36μm to M71-B (3600/0.33/-0.7) we got $S = 583$ (log N(C)= -5.38, $^{12}C/^{13}C$ =5), whereas for the extended region 2.285 — 2.378μm we obtained a less good minimisation of $S = 664$ (log N(C) = -5.38, $^{12}C/^{13}C$ =3), see left panel of Fig. 8.

(3) We obtained the same log N(C) from the fit to the extended region because the main contribution to S was provided by strong ^{12}CO bands which are common in both cases. When this is not the case or when edge effects are evident our results for the $^{12}C/^{13}C$ ratio become very sensitive to the quality of spectrum on the redward side of the 2.375 μm band.

(4) Carbon isotope ratios are systematically lowered, if we use 2.36-2.38μm for our analysis (see table 1 for three M71 giants).

(5) In the right panel of Fig. 8 we show another example of a fit to M13-II-76 (4202/1.10/-1.4). In that case the fit was performed to the narrower wavelength region. The measured flux at wavelengths greater than 2.36 μm is significantly lower than the theoretical values. Furthermore, without a sophisticated normalisation we get a non-physical $^{12}C/^{13}C < 3$ if we fit to the 2.285-2.38μm region.

We conclude that the use of the second band-head of $^{13}C^{16}O$ at 2.375 μm in our analysis degrades rather than improves our results. Due to its poorer signal-to-noise ratio and the possibility of non-optimal extraction at the end of the spectrum, we excluded it from our analysis.

4 RESULTS

Results of log N(C) and $^{12}C/^{13}C$ determinations for our giants are shown in Table 2. Before addressing each cluster we mention some other general results. First of all, in Table 3 we list objects for which there are C and $^{12}C/^{13}C$ abun-

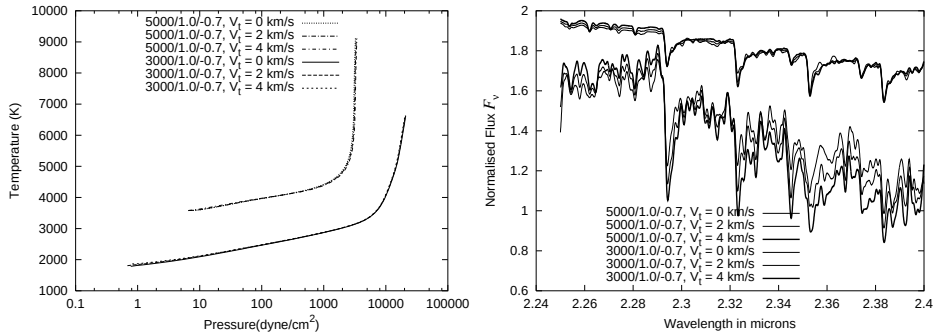

Figure 7. Computed temperature structures and the synthetic spectra for different V_t ($^{12}C/^{13}C = 3$ for all models).

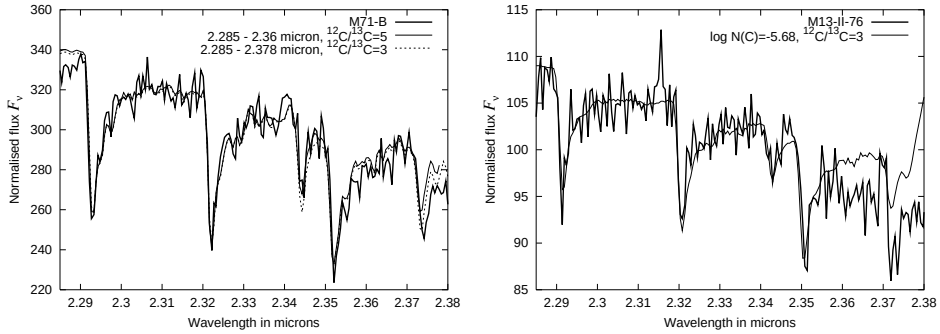

Figure 8. Left: Fits to observed spectra Fits to observed spectra for the full spectral region for M71-B (left) and M13-II-76 (right).

dance values in the astronomical literature, along with our log N(C) and $^{12}C/^{13}C$ determinations. In general, within the errors of our spectra and procedure our carbon abundances are consistent with those of giants with known carbon and oxygen abundances. Then, to study the impact of variations in some of our other input parameters we carried out some numerical experiments:

- To test the dependence of our results on V_t we carried out some additional modelling of our M5 giant spectra. We determined log N(C) and $^{12}C/^{13}C$ for them adopting different V_t . Our results are shown in Table 4. They show that the models are very sensitive to the value of V_t . We are able to determine individual values of V_t for given giants: namely, V_t = 2 km/s for M5-II-9 and M5-IV-81, V_t = 3 km/s for M5-IV-59.
- In the last two columns of Table 4 we show the dependence of our results on T_{eff} . Effective temperatures of all stars were increased by 100 K and the fitting procedure was repeated. It can be seen that our results, i.e. log N(C) and $^{12}C/^{13}C$, remain in the frame of our error bars, i.e. ± 0.2 dex and ± 1, respectively.

4.1 M71 (NGC 6838)

Globular cluster M71 is a nearby metal-rich cluster. Sneden et al. (1994) found for M71 some evidence of star-to star differences in O (and Na) abundances. Briley et al. (1994, 1997) carried out isotopic carbon abundance analysis using fits of weak ^{12}CN and ^{13}CN bands in spectra at 800.2-800.6 nm across a narrow range of effective temperatures (4000-4350 K). Ramirez & Cohen (2002a) performed an extensive analysis of abundances in atmospheres of red giants and subgiants of M71 based on the optical and near-infrared spectra. There is no overlap in objects or in spectral region between these studies and ours.

The cluster lies in a relatively crowded field at low galactic latitude. From the proper motion study results of Cudworth (1985) we found that at least four stars of our sample are non members of M71. The membership probabilities for stars N, A5, A7, A6 are of 0 %, 6 %, 0%, 10 %, respectively. M71-79 has a 51 % probable membership. Our determination of log N(C) and $^{12}C/^{13}C$ for the field stars should be considered as indicative not qualitative results, in part because we fix their metallicity as [μ] = –0.7. Nevertheless, analysis of the whole sample of stars enabled us to confirm that we can indeed see differences between cluster and field stars.

Our fits to the observed spectra of M71 giants are given in Fig. 9, fits to the field star spectra are shown in Fig.10. In general, the fits are of good quality. Only fits to spectra with the poorest signal-to-noise ratio, the hottest giants 'N' and 'C', cause problems. The membership probability of M71-C is 95 % (Cudworth 1995) and the 'best' solutions suggest too a high value of $^{12}C/^{13}C$ =90. Perhaps we are seeing some peculiarities in the chemical abundance of this star. This relatively hot (and faint) giant should be studied in more detail.

Non-member M71-N is explained more simply. We obtained a fit for a carbon-rich atmosphere with low $^{12}C/^{13}C$, though this probably results from incorrect input data —

Table 1. Carbon abundances and $^{12}C/^{13}C$ in giants of M71 from the fits to 2.285 — 2.36 and 2.285 — 2.38 μm

			2.285 — 2.36 μm			2.285 — 2.38 μm		
Cluster	Object	T_{eff} /log g	log N(C)	$^{12}C/^{13}C$	S	log N(C)	$^{12}C/^{13}C$	S
M71	b	3600/0.33	-5.38	5	583	-5.38	3	664
	30	3925/0.88	-4.38	7	420	-4.38	4	688
	21	4349/1.65	-4.38	5	467	-4.38	3	642

Table 2. Derived values for [C] and $^{12}C/^{13}C$ are given. Values of metallicity, temperature and gravity are taken from Alonso et al. (1999, 2000). Data was also taken of i61 in M5 and I-21 and IV-59 in M13, however, the S/N of the data is rather poor and so data for these objects is not included. Cluster non-members as determined by proper motions studies are given in italics.

Cluster	[Fe/H]±0.1	Object	log ($L/L_\odot$)	T_{eff}	log g	log N(C)	[C] ±0.1	$^{12}C/^{13}C$
M71 members	–0.71	21	2.33	4349±48	1.65	–4.38	-0.19	5±2
		30	2.84	3925±56	0.88	–4.38	-0.19	7±2
		B	3.08	3600±72	0.33	–5.38	-1.19	5±3
		29	3.19	3574±50	0.09	–4.58	-0.39	9±2
		C, noise	2.08	4856±60	2.51 –3.78	+0.41	95±10	
M71 non-member?		79?	1.80	4556±56	2.20	–3.98	+0.36	5±2
M71 non-members	–0.71	*N*, noise	*1.99*	*4840±60*	*2.12*	*–2.82*	*+1.37*	*3±1*
		A5	*1.86*	*4531±57*	*2.10*	*–4.18*	*+0.01*	*10±3*
		A7	*2.04*	*4411±53*	*1.92*	*–4.38*	*-0.19*	*20±5*
		A6	*2.70*	*3897±72*	*1.02*	*–4.18*	*-0.01*	*20±5*
M5	–1.3	IV-59	2.90	4243±45	1.0	-5.38	-0.6	7±3
		II-9	3.03	4230±48	0.9	-5.58	-0.8	3±1
		IV-81	3.23	3963±53	0.6	-5.58	-0.8	4±1
M13		I-24, noise	2.61	4374±57	1.10	-5.58	-0.5	5±5
	–1.4	II-76	2.87	4202±52	1.10	-5.58	-0.7	3±1
		III-73	2.99	4164±52	0.90	-5.58	-0.7	3±1
		III-56, noise	3.13	4013±41	0.70	-6.08	-1.0	7±2
		I-48, noise	3.21	3929±45	0.60	-6.68	-1.8	90±20
		II-67	3.28	3894±45	0.50	-6.38	-1.5	4±1
M3	–1.6	I-21	2.91	4124±52	1.0	-5.58	-0.5	4±1
		III-28	3.03	4092±43	0.8	-5.78	-0.7	4±1
		AA	3.12	3977±50	0.7	-5.78	-0.7	3±1
		II-46	3.12	3951±52	0.7	-5.58	-0.5	4±1
M3 non-member?		1397?	3.15	3916	2.5	-4.72	+1.3	5±1

at least the spectrum belongs to a cooler star with low $^{12}C/^{13}C$.

We found a similar picture for M71-79 — even with [C/Fe] = 0.36, we do not reach a minimum in S. Most probably, star 79 is not member of M71.

The values of log N(C) and $^{12}C/^{13}C$ determined for our M71 sample are given in Table 2. We find:

- Giants of M71 show $^{12}C/^{13}C$ =6 ± 3; this dispersion is generally consistent with observational errors.
- The dispersion of $^{12}C/^{13}C$ in the atmospheres of M71 giants is smaller than in the M71 non-members sample.

4.2 M5 (NGC 5904)

M5 is a mildly metal-poor cluster ([Fe/H]= -1.4, Zinn & West 1984, [Fe/H]=-1.11, Sneden et al. 1992; [Fe/H]=-1.1 Caretta & Gratton 1997). From analysis of 36 giants in M5 Ivans et al. (2001) found no significant abundance variations for Mg, Si, Ca, CS, Ti, V, Ni, Ba and Eu. However, large variations were found for abundances of O, Al, Na, which are sensitive to the proton-capture nucleosynthesis. Recently Cohen et al. (2002) carried out abundance analysis for stars at the base of the red giant branch (RGB) of M5. Star-to-star variations with a significant range in both [C/Fe] and

Table 3. Comparison with literature values for target objects: M5 from Ivans (2001), M3-IV-59 Smith et al.(1997), M13 from Smith et al. (1996), M13 from Kraft et al. (1997).

Cluster	Object	Fe/H	lit [O]	lit [C]	our [C]
M5	IV-59	-1.25–1.40	+0.37	-0.6^{sm}	-0.5
M3	AA	-1.45	-0.22	-1.15^{s}	-1.0
	III-28	-1.49	0.31	-0.88^{s}	-0.8
	II-46	-1.46	0.29	-0.84^{s}	-0.7
M13	III-56	-1.51	-0.02	-1.19^{s}	-1.2
	III-73	-1.51	0.34	-0.86^{s}	-0.8
	II-67	-1.51	-0.64, -0.79^{k}	-1.34^{s}	-1.45
	II-76	-1.49	0.46	-0.82^{s}	-0.9
M13	I-48	-1.57	-0.75		-1.8
	II-67	-1.52	-0.79		-1.6

^{s} — Smith et al. (1996)
^{sm} — Smith et al. (1997)
^{k} — Kraft et al. (1997)

Table 4. Dependence of log N(C) and $^{12}C/^{13}C$ on metallicity, microturbulent velocities and temperatures for M5 giants. Below the pairs log N(C)/$^{12}C/^{13}C$ the (S) values are given(see Section 3)

			$[\mu]/V_t/\Delta T$			
Giant	-1.13/1/0	-1.13/2/0	-1.13/3/0	-1.13/4/0	1.11/2/0	-1.11/2/+100
II-9	-5.36/5	-5.58/3	-5.58/3	-5.58/3	-5.58/3	-5.38/3
	(937)	(912)	(929)	(957)	(926)	(916)
IV-59	-4.98/20	-5.38/7	-5.38/5	-5.38/2	-5.18/8	-5.18/8
	(538)	(509)	(500)	(529)	(515)	(503)
IV-81	-4.98/10	-5.58/5	-5.78/4	-5.79/3	-5.58/5	-5.38
	(414)	(379)	(408)	(410)	(377)	(394)

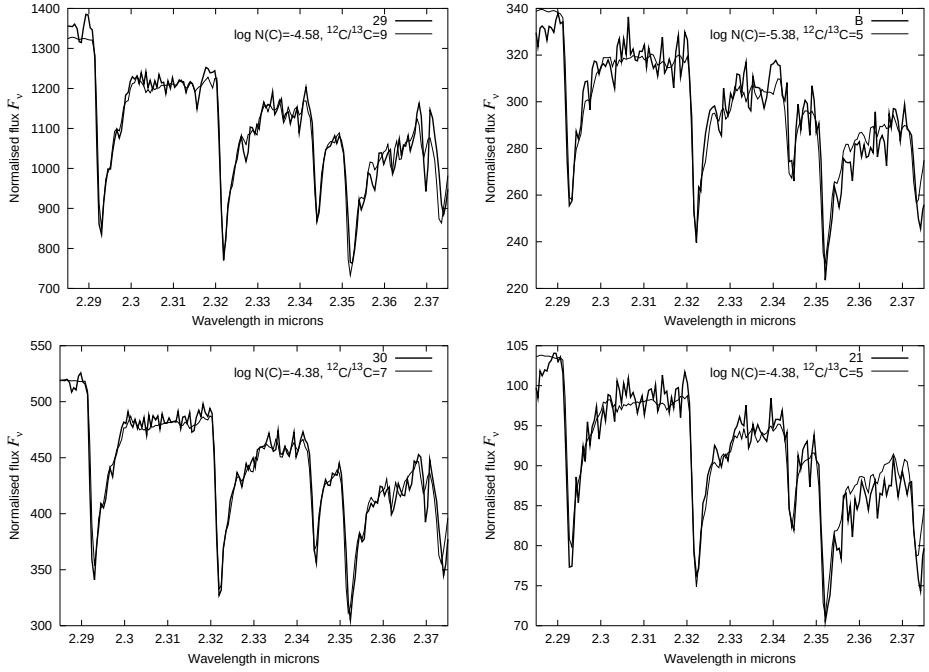

Figure 9. Fits to observed spectra of M71 giants arranged by effective temperatures.

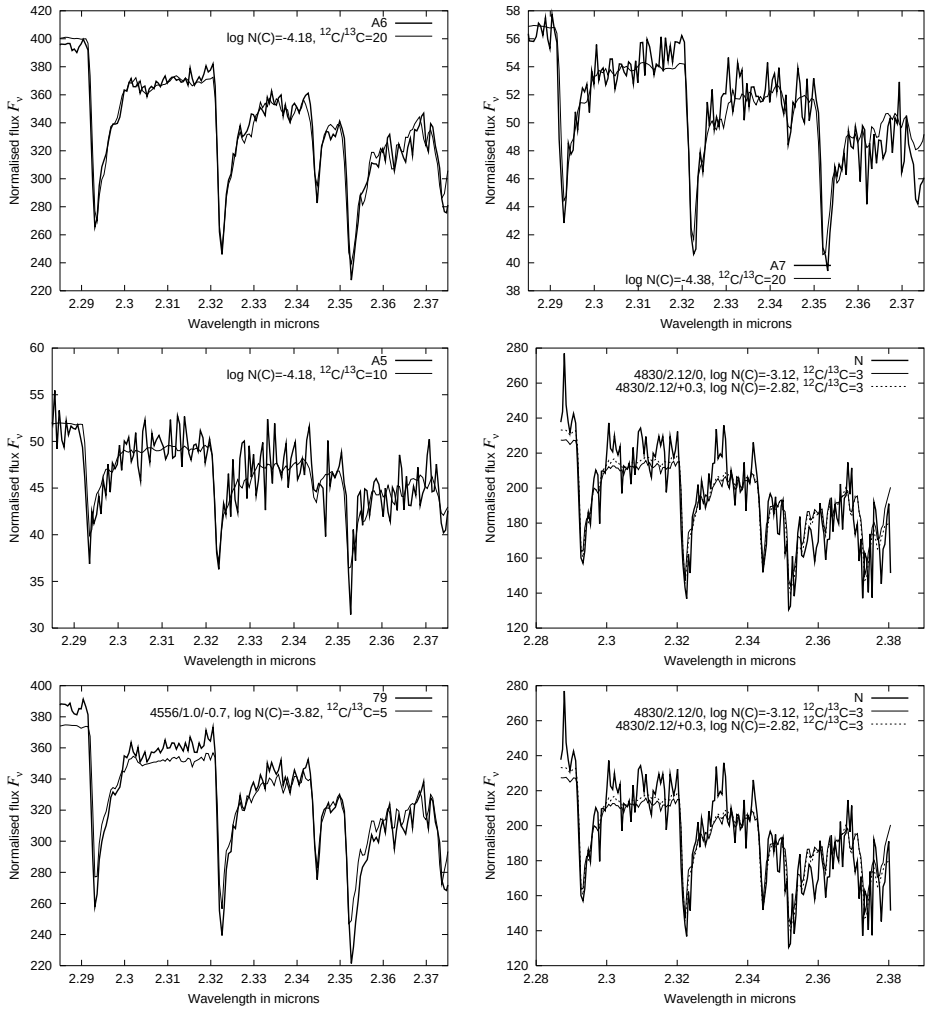

Figure 10. Fits to observed spectra of field stars of our "M71 sample" arranged by effective temperatures.

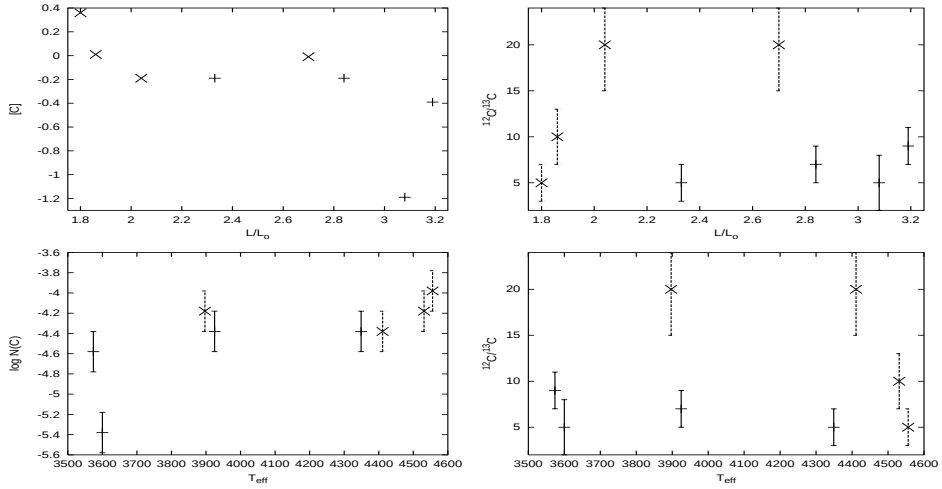

Figure 11. The interdependence of carbon abundance (log N(C)), isotopic ratio (^{12}C/^{13}C), effective temperature ($T_{\rm eff}$) and luminosities (LŁ$_o$) for "M71 sample" giants: cluster members (+), field stars(×)

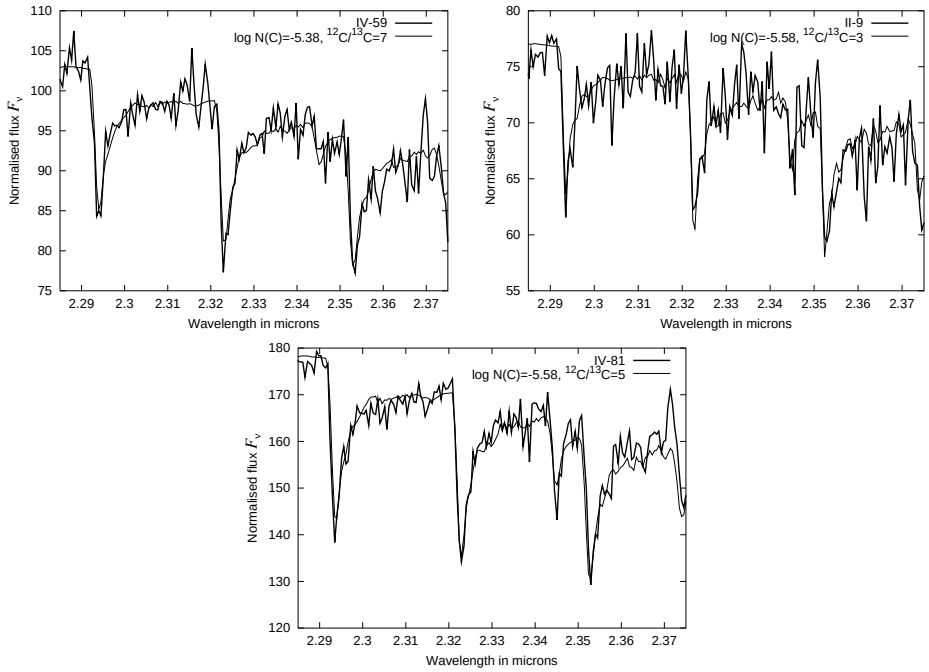

Figure 12. Fits to observed spectra in M5.

[N/Fe] are found at all luminosities extending to the bottom of RGB at $M_v \sim 3^m$.

Giants IV-59 and II-9 are members of M5 (99 % probability, Cudworth 1979); for IV-89 membership is not yet established from proper motion measurement. However the results of log N(C) and $^{12}C/^{13}C$ determinations for M5-IV-89 agree well with those for the established members IV-59 and II-9 (see table 2). We conclude that we have confirmed the membership of M5-IV-89 spectroscopically.

Our fits to the observed spectra of M5 giants are shown in Fig 12. In all cases we can find reasonable fits. [C/Fe] < – 0.6 in all the giants we measured.

We used the data for the M5 giants to carry out an additional test, on the sensitivity to metallicity of the carbon abundance we derive. We performed sets of computations for two metallicities, $[\mu]$ = -1.1 and $[\mu]$ = -1.3. All model atmospheres and synthetic spectra were re-computed for these abundance grids. Results are given in Table 5. The changes in isotopic ratio $^{12}C/^{13}C$ and carbon abundance log N(C) deduced indicated that the uncertainty in metallicity introduced errors of only ± 1 and ± 0.2 dex, respectively.

We found a comparatively high $^{12}C/^{13}C$ = 7 ratio in giant IV-59. Its atmosphere is moderately deficient in carbon compared to the other giants in M5. However, the spectrum of IV-59 is relatively noisy. Also, our experiments with V_t show that $^{12}C/^{13}C$ =5 ± 2 for V_t = 3 km/s for this star (see table 4).

4.3 M13 (NGC 6205)

Kraft et al. (1997) studied abundances of O, Na, Mg and Al in giants of M13 ([Fe/H] = -1.5). Briley et al. (2002) found that M13 is distinguished by rather large star-to-star variations in carbon (and possibly other light elements).

All stars of our sample are members of M13 with probability 99 % (Cudwotrh 1979a). The fits to M-giants spectra of M13 are presented in Fig 13. The spectrum of M13-I-18 is too noisy to permit any reliable analysis and spectra of M13-III-56, M13-I-48, M13-I-24 are also noisier than for our other giants.

Fig. 14 shows a negative slope in the dependence of log N(C) on f($L/L_\odot$). This result was found by other authors for different clusters (e.g., Briley et al. 2002 and references therein). In the atmospheres of the majority of M13 giants $^{12}C/^{13}C < 10$.

A few determinations of log N(C) for some giants of M13 are known from the literature. In general, our determinations agree with them well (see table 3).

4.4 M3 (NGC 6272)

Globular cluster M3 is the most metal deficient from our sample ($[\mu]$ = –1.6). According to Cudworth (1979b), all our stars are members of M3 (with probability 99 %), except for 1397. We found a carbon-rich solution for this star, which seems to be an artefact (like M71-N and M71-79), most probably caused by adopting (incorrectly) a metallicity the same as that of the cluster.

Fits to observed spectra are shown in Fig. 15. Our sample of giants has a small range of temperature around 4000K though a large range of log N(C) from –5.58 to –6.08. Nonetheless all have a very similar $^{12}C/^{13}C$ ratio of 4 — 5. Our carbon abundance determinations agree well with the M3 giants in the list of Smith et al. (1997).

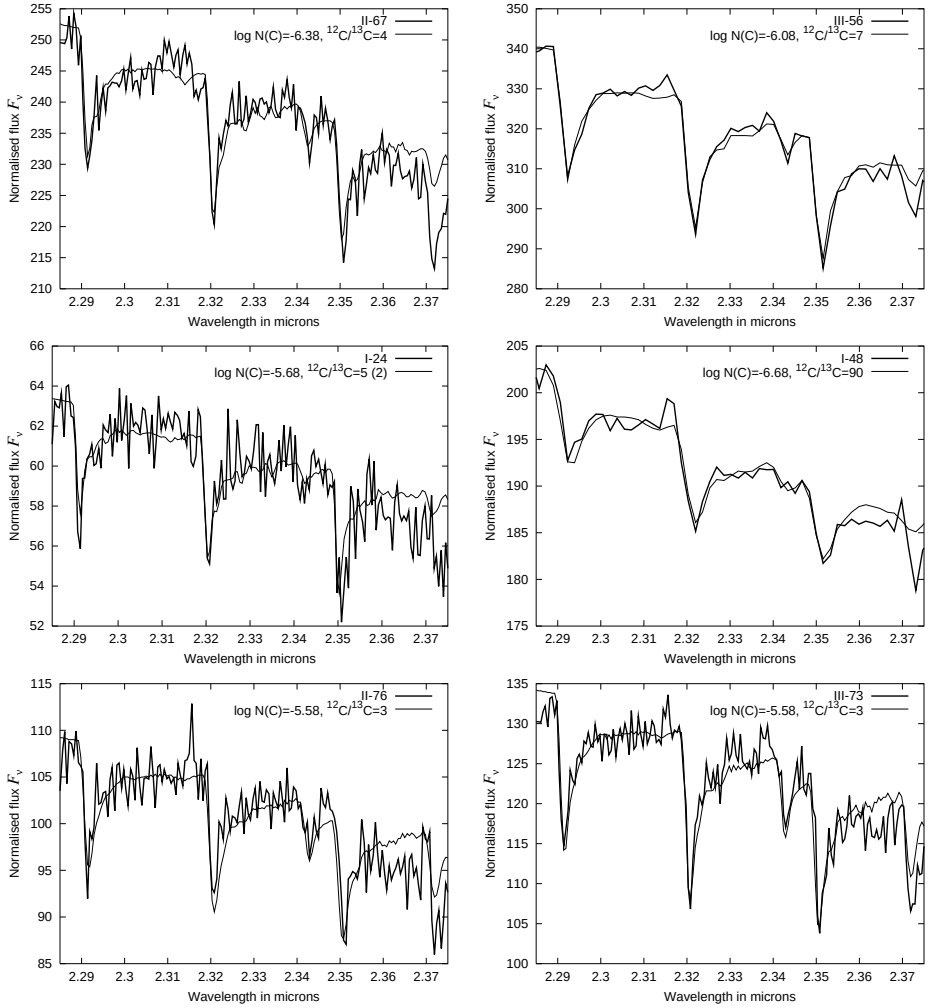

Figure 13. Fits to the observed spectra in M13.

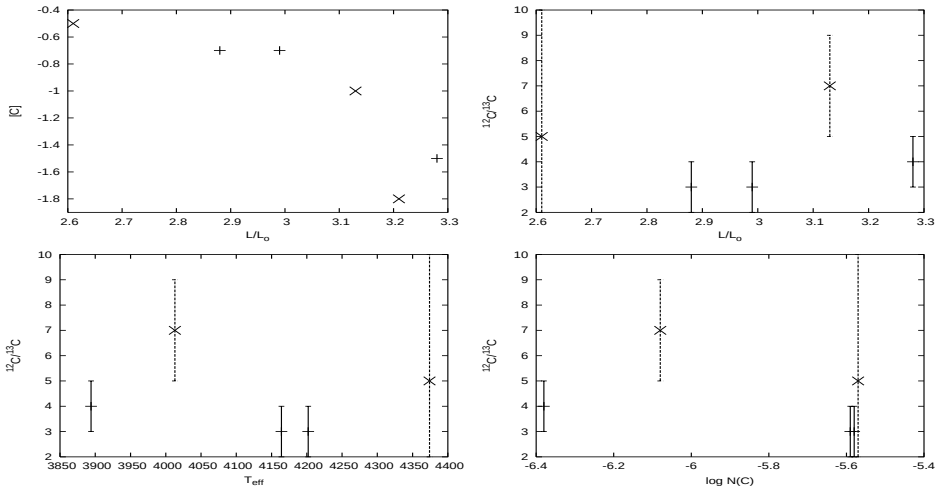

Figure 14. The interdependence of carbon abundance (log N(C)), isotopic ratio (^{12}C/^{13}C), effective temperature ($T_{\rm eff}$) and luminosities (LŁ$_o$) for M13 giants. Resylts for more and less confident spectra are showed by (+) and (×), respectively.

Table 5. Carbon abundances in giants of M5 computed for model atmospheres of [μ] = 1.1 and -1.3.

			[μ]=-1.3			[μ]=-1.1		
Cluster	Object	T_{eff} /log g	log N(C)	[C/Fe]	$^{12}C/^{13}C$	log N(C)	[C/Fe]	$^{12}C/^{13}C$
M5	IV-59	4343/1.0	-5.38	-0.6	7	-5.18	-0.6	8
	II-9	4320/0.9	-5.58	-0.8	3	-5.58	-1.0	3
	IV-81	3963/0.6	-5.58	-0.8	5	-5.58	-1.0	5

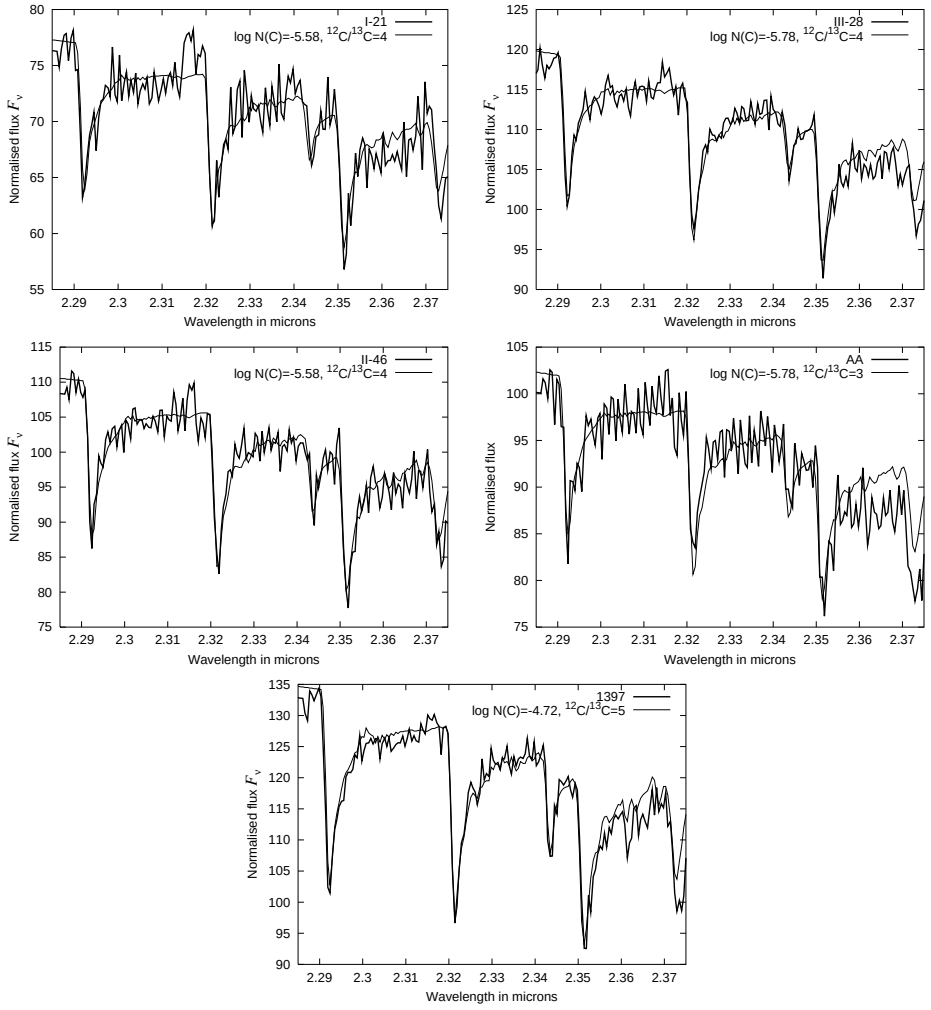

Figure 15. Fits to observed spectra in M3.

5 DISCUSSION

We have analyzed photospheric carbon isotope ratios for a sample of 25 giants in different galactic globular clusters using fits to infrared spectra dominated by H_2O and CO bands in the wavelength range 2.28–2.39 μm . We used T_{eff} and log g values from Alonso et al. (1999) and cluster metallicities from the literature. Effective temperatures in Alonso et al. are given with an accuracy of $< \pm$ 100 K. Our numerical experiments indicate that with this level of uncertainty our results remain inside our empirical error bars: $\pm$ 0.2 and 1 for carbon abundance and $^{12}C/^{13}C$ respectively in the atmospheres of the majority of our giants.

In our analysis we used model atmospheres computed using a classical approach with opacity sampling treatments of the absorption by atomic and molecular lines. Comparison of our models with NEXTGEN oxygen rich model atmospheres (Hauschildt at al. 1999) and carbon-rich models of Erikson (1994) shows good agreement (Pavlenko 2002, 2003). For the most luminous giants the plane-parallel models may be not valid. Nevertheless, due to the lower opacities in the atmospheres of metal-deficient stars, their photospheres move toward higher pressure regions, in which sphericity effects should be smaller. Therefore we believe that our results would not change significantly if analysed with model atmospheres computed taking sphericity

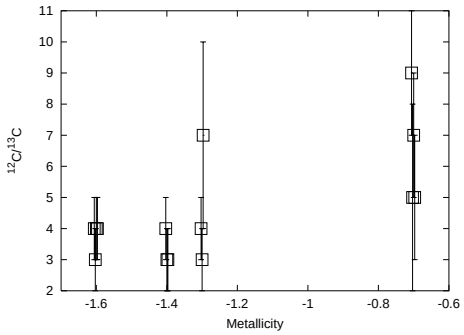

Figure 16. Isotopic ratios $^{12}C/^{13}C$ in giants of different clusters. Two giants with $^{12}C/^{13}C > 90$ are not showed to simplify the plot.

effects into account. We also note that for luminous stars we should in principle compute effects caused by mass loss processes, i.e. stellar wind, peculiar convection processes, inhomogeneities of their photospheres. In practice, consideration of these effects lies beyond the scope of this paper.

Although nitrogen and oxygen abundances can vary in the atmospheres of globular cluster giants, initially we set fixed abundances of oxygen and nitrogen. Our numerical experiments (section 4) then indicated that the dependence of our results on the adopted value of log N(C) is much stronger than the dependence on log N(O). This may be understood in terms of molecular abundances – N(O) >> N(C), and N(CO) >> N(CN) in our cases. We did not try varying the abundance of nitrogen because there were no transitions involving nitrogen in our spectra.

Our carbon abundances are in good agreement with other authors despite the different numerical procedures inherent to the various models. We therefore confirm the deficiency in carbon abundances and the general nature of low $^{12}C/^{13}C$ in the atmospheres of the giants of globular clusters. We determined log N(C) and $^{12}C/^{13}C$ for relatively luminous giants which are above the bump of luminosity function. We note that an increase of $^{12}C/^{13}C$ with decreasing luminosity towards the bump has been observed for giants in M4 and NGC 6528 (Shetrone 2003). In general, our results are also in good qualitative agreement with the theoretical predictions of Boothroyd & Sackman (1999) for the connection of the surface abundances and the still hypothetical deep circulation mixing below the base of the standard convective envelope and the consequent "cool bottom processing" of CNO isotopes. We note that in these theories of the final stage of evolution of a single star, a number of important parameters remain poorly known. These include mass loss, rotation rates (see Denissenkov et al. 1997 and reference therein), the temperature difference between the bottom of mixing and the bottom of H-burning shell (Boothroyd & Sackman 1999).

Some mechanisms that have been suggested to transport evolved matter into the surface layers include:
a) meridional circulation driven by rotation of the interior (Sweigart and Mengel 1979),
b) turbulent diffusion processes (Bienayme et al 1984, Denissenkov & Weiss 1996),
c) deep circulation mixing (Boothroyd & Sackman 1999).
In general the efficiency of such mixing mechanisms depends on the individual characteristic of each star — rotation, multiplicity, etc. Moreover, the problem is complicated by the need to take into account a contribution from pollution processes on the early stages of evolution of globular clusters, which have their own history.

6 CONCLUSIONS

We confirm the results of previous observational studies that the $^{12}C/^{13}C$ ratio in metal-poor stars is a factor of 3-5 lower than predicted by standard models of low-mass stellar evolution that do not include mixing beyond the first dredge-up.

• Within both M3 and M13, with $[\mu] <$ - 1.3, the giants we observed have about the same $^{12}C/^{13}C$ ratio.

• Fig. 16 provides some evidence for lower $^{12}C/^{13}C$ in giants of globular clusters of lower metallicity. This result was predicted by theory. Indeed, all theories of mixing to date predict a metallicity dependence for mixing efficiency - the molecular weight gradient/barrier will be steeper with increasing $[\mu]$ and the H-shell will be hotter/wider with decreasing $[\mu]$, so a plot like Fig. 16 was expected.

• Giants of more metal-rich clusters show larger dispersion of $^{12}C/^{13}C$ (see Table 2).

• More evolved red giants with lower log g (< 1) show reduced log N(C).

Our measurements confirm the conclusions of work on field giants. However, the carbon isotope ratios of the most evolved population I giants are even lower than our typical values of $^{12}C/^{13}C = 4 - 9$. Nevertheless, our data in concert with carbon isotope ratios measured in other studies, for field and cluster stars spanning a large range of metallicities, illustrate the existence of an unidentified extra mixing processes inside globular cluster giants after the the first dredge-up event. To distinguish when this process begins it is important to conduct similar measurements on less evolved stars in these clusters.

ACKNOWLEDGMENTS

We thank our anonymous referee for a very helpful review of the paper. This work was partially supported by a PPARC visitors grants from PPARC and the Royal Society. YPs studies are partially supported by a Small Research Grant from American Astronomical Society. We thank David Schwenke and David Goorvitch (AMES) for

providing H_2O and CO line lists in digital form and Roger Bell and Paul Butler for useful discussions.

This research has made use of the SIMBAD database, operated at CDS, Strasbourg, France.

REFERENCES

Alonso, A., Arribas, S., Martinez-Roger, C, 1999, A&AS., 139, 335.
Alonso A., Salaris M., Arribas S., Martinez-Roger C., Asensio Ramos A. 2000, A&A, 355,1060.
Anders, E. & Grevesse, N. 1989, Geochimica et Cosmochimica Acta, 53, 197.
Asida, S.M. 2000 ApJ 528, 896.
Bell, R.A., Briley, M.M. 1991, AJ, 102, 763.
Bienayme, O., Maeder, A., Schatzman, E. 1984, A&A, 131, 316.
Boothroyd, A.I., Sackman, I-J. 1999, ApJ, 510, 232.
Boyarchuk, M. E., Pavlenko, Y. V., Shavrina, A. V. 1991. Sov. Astron., 35, 143.
Briley, M.M., Smith, V.V., Lambert, D.L., 1994, ApJ, 429, L119.
Briley, M.M., Smith, V.V., King, J., Lambert, D.L. 1997, AJ, 113, 306.
Briley, M.M., Cohen, J.G., 2001, AJ, 122, 242
Briley, M.M., Smith, C.H., Claver, C.F. 2001, AJ, 122, 2561.
Briley, M.M., Cohen, G.C., Stetson, P.B. 2002, ApJ, 579, L17.
Caretta, E. & Gratton, R.G. 1997, A&AS, 121, 95.
Charbonnel, C., 1994, A&A, 282, 811.
Cottrell, P. L., 1978. Apj, 223, 544
Cudworth, K.M., 1979, AJ, 84, 1866.
Cudworth, K.M., 1979a, AJ, 84, 1866.
Cudworth, K.M., 1979b, AJ, 84, 1312.
Cudworth, K.M., 1985, AJ, 90, 65.
Denissenkov, P.A., Weiss, A. 1996, A.A. 1996, A&A, 308, 773.
Doyle, R.O. 1968, ApJ, 153, 987.
Gilroy, K.K., Brown, J.A., 1991, ApJ, 371, 578.
Cohen, J.G., Briley, M.M., Stetson, P.B. 2002, AJ, 123, 2525.
Eriksson, K., Gustafsson, B., Jørgensen, U. G., and Nordlung, Å. 1984. A&A, 132, 37.
Goorvitch, D. 1994, Ap.J.Suppl.Ser., 95, 535.
Gratton, R.G., Bonifacio, P., Bragaglia, A., Carretta, E., Castellani, V., Centurion, M., Chieffi, A., Claudi, R., Clementini, G., D'antona, F., Desidera, S., Francois, P., Grundahl, F., Lucatello, S., Molaro, P., Pasquini, L., Sneden, C., Spite, F., Straniero, O. 2001, A&A, 369, 87.
Hauschildt, Peter H.; Allard, F., Baron, E. 1999, ApJ, 512, 377.
Heiter, U., Kupka, F., van't Veer- Menneret, C., Barban, C., Weiss, W. W., Goupil, M.-J., Schmidt, W., Katz, D., Garrido, R. 2002, A&A, 392, 619
Iben, Jr.I., Renzini, A. 1983, ARA&A, 21, 271.
Iben, Jr.I. 1964, ApJ, 140, 1631.
Ivans, I.I., Kraft, R.P., Snenen, C., Smith, G.H., Rich, R.M., Shetrone, M. 2001, AJ, 122, 1438.
Jones, H.R.A., Longmore, A. J., Jameson, R. F., Mountain, C. M., 1994, MNRAS, 267, 413
Jones, H.R.A., Pavlenko, Y.V., Tennyson, J., Viti, S. 2002, MNRAS, 330, 675.
Kraft, R.P., Sneden, C., Langer, G.E. & Prosser, C.F. 1992, Astron. J., 104, 645.
Kraft, R.P. 1994, PASP, 106, 553.
Kraft, R.P., Sneden, C., Smith, G.H., Shetrone, M.D., Langer, G.E., Pilachowski, C.A. 1997, AJ, 113, 279.
Kupka, F., Piskunov, N., Ryabchikova, T. A., Stempels, H. C., Weiss, W. W. 1999. A&A Suppl., 138, 119.
Kurucz, R.L., 1993, CD-ROM 18.
Kurucz, R.L., 1999. http://cfa5.harvard.edu
Lambert, D.L., Ries, L.M. 1981. ApJ, 248, 228.
Malkan M.A., Hicks E.K., Teplitz H.I., McLean I.M., Sugai H., Guichard J., 2002, ApJS, 142, 79
Myerscough, V. 1968, ApJ, 153, 421.
Messenger, B.B., Lattanzio, J.C. 2002, MNRAS, 331, 684.
Pavlenko, Y. V. 1991. Sov. Astron., v.35, p.212.
Pavlenko, Ya.V. 1997. Astrophys. Space Sci., 253, 43.
Pavlenko, Ya. V. 2000. Astron. Rept. 44, 219
Pavlenko, Y. V. 2002. Proc. of IAU210, Uppsala, ed. N.Piskunov, in press (astro-ph 0209022).
Pavlenko, Y.V., Jones, H.R.A. 2002. A&A., 396, 967.
Pavlenko, Y. V. 2003. Astron. Rept., 47, 59.
Pavlenko, Ya.V. & Zhukovska, S.V. 2003, Kimemat. Phys. Celest. Bodies, 19, 28.
Pavlenko, Ya.V. 2003b, http://www.mao.kiev.ua/staff/yp/Results/CNO_bf.tar.gz
Ramirez, S.V., Cohen, J.G. 2002, Astron. J., 123, 3277.
Ramirez, S.V., Cohen, J.G. 2002a, Astron. J., 125, 224.
Partrige, H., Schwenke, D.J. 1997, Chem. Phys. 106, 4618.
Salaris, M., Cassisi, S., Weiss, A., 2002, PASP, 114, 375.
Schwenke, D.J. 1997. http://george.arc.nasa.gov/~dschwenke
Pilachowski, C., Sneden, C., Hinkle, K., Joyce, R. 1997, AJ, 114, 819.
Seaton, M.J., Zeipen, C.J., Tully, J.A. 1992, Rev. Mexic. Astron. Astrophys. 23, 107.
Shetrone, M.D. 2003, ApJ, 585, L45.
Smith,V.V., Suntzeff, N.B. 1989, AJ, 97, 1699.
Smith, G.H., Schetrone, M.D., Bell, R.A., Churchill, C.W., Briley, M.M. 1996, AJ, 112, 1511.
Smith, G.H., Shetrone, M.D., Briley, M.M., Churchill, C.W., Bell, R.A. 1997. PASP, 109, 236.
Smith, V.V., Suntzeff, N.B., Cunha, K., Allino, R., Busso M., Lambert, D.L., Straniero, O. 2000, AJ, 119, 1239.
Smith, G.H. 2002, PASP, 114, 1097.
Smith, G.H., Terndrup, D.M., Suntzeff, N.B. 2002, AJ, in press (astro-ph 020743).
Sneden, C.; Johnson, H. R.; Krupp, B. M. 1976, ApJ, 204, 218.
Sneden, C., Pilachovski, C.A. and VandenBerg, D.A. 1986, ApJ, 311, 826.
Sneden, C., Kraft, R,P., Prosser, C., Langer, G.E. 1992, AJ, 104, 2121.
Sweigart, A.V., & Mengel, J.G. 1979, ApJ, 229, 624.
Tsuji, T. 1973 A&A, 23, 411.
Unsold, A. 1955. Physik der Sternatmospharen, springer Verlag, 2-nd ed.
Vanture, A.D., Wallerstein, G., Suntzeff, N.B. 2002, ApJ, 569, 984.
Yakovina, L.A. & Pavlenko, Ya. V. 1998, Kimem. Phys. Celest. Bodies, 14, 195.
Zinn, R. & West, M.J. 1984 ApJS, 55, 45.

This paper has been typeset from a TEX/ LATEX file prepared by the author.